STUDIA UBB CHEMIA, LXX, 2, 2025 (p. 149-161)
(RECOMMENDED CITATION)
DOI:10.24193/subbchem.2025.2.10

GOLD-DECORATED TITANIA NANOTUBES WITH GRAPHENE FOR VISIBLE LIGHT-MEDIATED AMOXICILLIN PHOTODEGRADATION

Alexandra URDA[a,b], Diana LAZAR[a], Dragos COSMA[a], Ion GROSU[b,*], Crina SOCACI[a,*]

ABSTRACT. The degradation of amoxicillin was accomplished using TiO_2 nanotubes photocatalysts decorated with Au nanoparticles and containing reduced graphene or nitrogen-doped graphene under visible light exposure. The structural and morphological characterization confirmed the presence of gold nanoparticles and graphene, and the optical properties showed light absorption into visible region. The best results in the degradation of amoxicillin (up to 60%) were reached in the presence of the photocatalyst with nitrogen-doped graphene. A basics kinetic study showed a physical adsorption of the amoxicillin on the catalyst surface, and that the photodegradation step followed the pseudo-first kinetic model with the apparent kinetic constant of 0.0039 min^{-1}.

Keywords: *amoxicillin, titania nanotubes, reduced graphene, nitrogen-doped graphene, photodegradation*

INTRODUCTION

The development of chemical and pharmaceutical industries led to a large release of industrial wastewaters into the environment, resulting in a growing deterioration of overall water. In an effort to reduce the chemical impact on public health and environmental quality, a wide range of technologies

---

[a] *National Institute for Research and Development of Isotopic and Molecular Technologies (INCDTIM), Donat 67-103 str., Cluj-Napoca, Romania.*
[b] *Babeş-Bolyai University, Faculty of Chemistry and Chemical Engineering, 11 Arany Janos str., RO-400028, Cluj-Napoca, Romania.*
[*] *Corresponding authors: crina.socaci@itim-cj.ro; ion.grosu@ubbcluj.ro*

are being employed based on *physical* (filtration, sorption techniques); *chemical* (precipitation, oxidation, irradiation, electrochemical processes) or *biological* (microbial degradation, enzymatic treatment) methods. However, these conventional wastewater treatment technologies still have some limitations (*e.g.* high operation costs, energy consumption, or reduce efficiency due to the chemical stability of reluctant pollutants [1]). In this context, photocatalysis is becoming a promising oxidation technique for an effective water and wastewater treatment, capable of degrading contaminants using UV and visible light exposure [2]. Even though a great amount of work has been performed in order to understand the mechanisms and improve the photodegradation efficiency of TiO_2-based nanomaterials [3], this oxide with semiconductive properties continue to be interesting for further development due to its low cost, high stability, availability and biocompatibility. Compared to nanoparticles, TiO_2 nanotubes (TiO_2NTs) are suggested to be superior in chemical and optoelectronic performance due to its one-dimensional channel for carrier transportation, in which the recombination of photogenerated e^-/h^+ is expected to be reduced.

Because the photonic efficiency of titanium dioxide is under 10% for majority of degradation processes [4] due to its restricted sensitivity to UV light [4-6], several methods for improvement has been proposed and developed: doping with 3d transition metals like Co, Ni, Mn, Fe [7] or noble metals, mainly silver or gold [8]; dye anchoring [9]; surface modifications [10]; and, in the last decade, the preparation of hybrids nanomaterials [11]. As part of our scientific interest, graphene showed their potential as electron co-catalyst to enhance the photocatalytic efficiency of semiconductors [12-18]. There is a common agreement regarding the positive impact of the graphene-based material [19,20], mainly based on their electron trapping properties or enhanced absorption capabilities. Further improvement in the photocatalytic activity has been demonstrated by the introduction of the heteroatoms (e.g. nitrogen) into the graphene sheet with altering the electronic structure thus shifting the photocatalytic response in the visible-light domain [21,22]. Previously, we investigated gold nanoparticles-decorated titania nanotubes photocatalysts with 10wt.% graphene oxide (GO) or reduced graphene oxide (TRGO), for the removal of β-estradiol under visible-light exposure [17].

Herein, we considered of interest to continue the investigations and prepare gold-decorated titania nanotubes (Au-TiO_2NT) with 10 wt.% and 20wt.% thermally reduced graphene oxide (TRGO) or nitrogen-doped graphene (NGr) and compare their visible-light-mediated photodegradation efficiency of amoxicillin as model pollutant. Amoxicillin is an antibiotic from the β-lactam family and was categorized in the emerging pollutant family due to its deleterious effects to the environment and human health, even at low concentrations [23,24].

RESULTS AND DISCUSSION

For the preparation of Au-TiO_2NT-TRGO/NGr we started with TiO_2 nanotubes obtained by hydrothermal treatment in an aqueous environment. The preparation of gold nanoparticles-containing titania nanotubes with reduced graphene oxide was employed by two methods and the structural features of the resulted composites were compared. In the first method, a mixture of TiO_2NT and graphene oxide (GO) was impregnated with thegold precursor, followed by a simultaneous thermal reduction of the metal and GO (Scheme 1). The second method was first decorating the TiO_2NT with Au nanoparticles, mixing with graphene oxide (GO), followed by graphene reduction (Scheme 2).

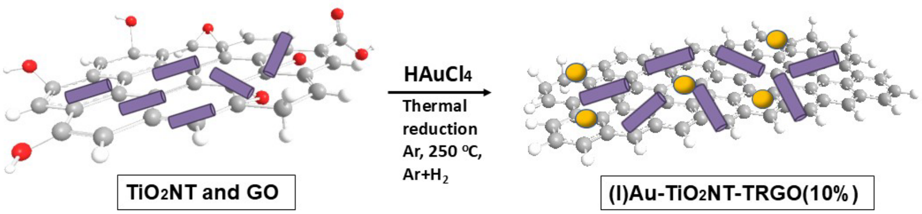

Scheme 1. Preparation method I for Au-TiO_2NT-TRGO composite (Au – gold nanoparticles; TiO_2NT - titania nanotubes; GO – graphene oxide; TRGO – thermally reduced graphene oxide)

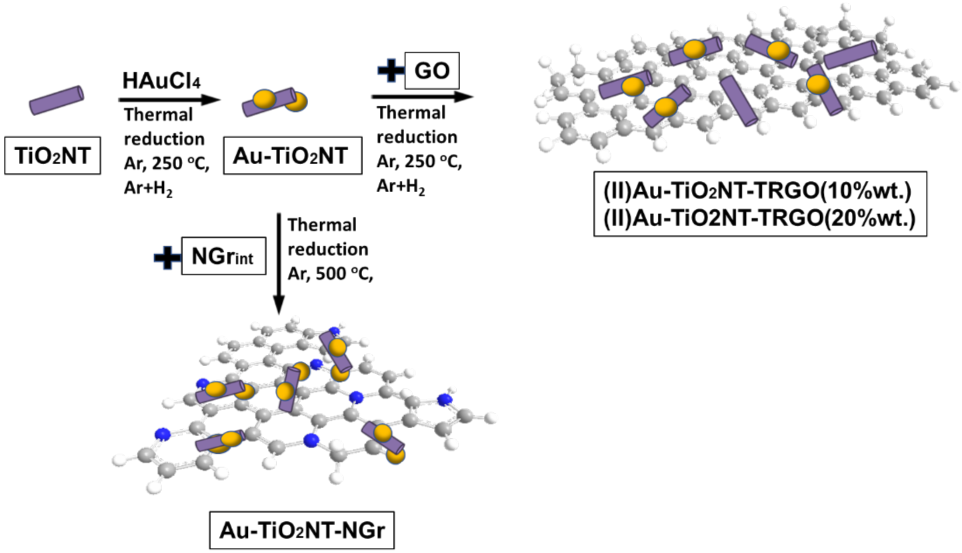

Scheme 2. Preparation method II for Au-TiO_2NT-TRGO composite and for Au-TiO_2NT-NGr (Au – gold nanoparticles; TiO_2NT - titania nanotubes; GO – graphene oxide; TRGO – thermally reduced graphene oxide; NGr – nitrogen doped graphene)

The nitrogen-doped graphene containing composite was obtained starting with the same titania nanotubes decorated with gold nanoparticles and mixing with a nitrogen-modified graphene oxide ($NGr_{int.}$) [18], followed by thermal annealing.

Structural and morphological characterization

Comparative X-Ray diffraction analysis showed that the TiO_2NTs are present only in the anatase form of titania in all the investigated nanomaterials (Figure 1). The comparison of the XRD spectra of Au(2.5wt.%)-TiO_2NT-TRGO catalysts prepared by the two methods (I or II) showed no significant differences. TRGO and NGr could not be observed in XRD patterns being covered by the intense reflection of anatase situated at 25.2°, so the general aspect of XRD patterns of Au(2.5wt.%)-TiO_2NT-graphene catalysts and of the corresponding Au-TiO_2NT are very similar. The three main reflections of metallic Au (30.1°, 44.3° and 64.4°) are well observed and suggest the presence of well crystalized metal with relatively large Au crystallites: 36 nm diameter for the first preparation method, and 16-20 nm for the second method.

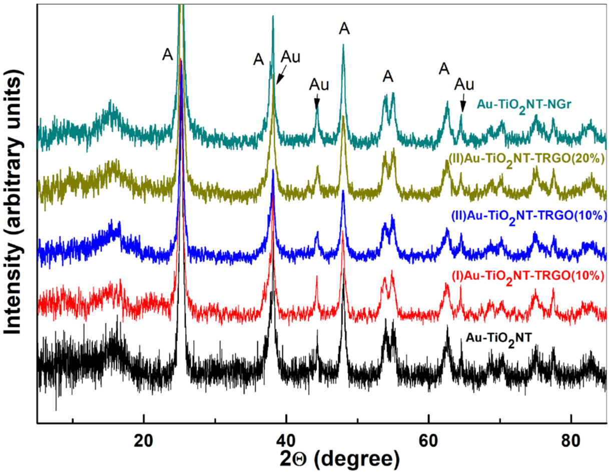

Figure 1. X-Ray diffractograms of the prepared photocatalysts powders (A – anatase)

The electronic microscopy (TEM) investigation confirms the presence of well dispersed large AuNPs (Figure 2) in the Au(2.5wt.%)-TiO_2NT-graphene catalysts prepared by all three methods. The TEM images show large Au nanoparticles of about 15-20 nm for the second method, confirming the calculated dimensions of the Au nanoparticles from XRD data.

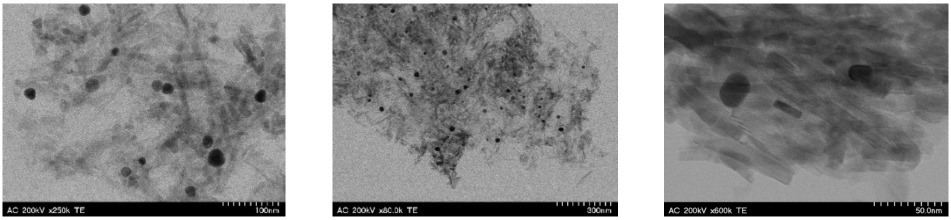

(II)Au-TiO_2NT-TRGO(10%) (II)Au-TiO_2NT-TRGO(20%) Au-TiO_2NT-NGr(20%)

Figure 2. TEM micrographs of selected photocatalysts decorated with Au NPs.

To conclude, the XRD and TEM characterization of materials showed no significant differences between these materials and the metal/TiO_2NTs catalysts, showing that graphene derivatives are not affecting the crystalline structure of gold-decorated titania nanotubes.

Optical properties of the prepared photocatalysts

UV–Vis reflectance spectra of the investigated Au-TiO_2NT-TRGO/NGr photocatalysts (Figure 3a) present the strong light absorption of TiO_2NT in the UV region due to the electron transfer from the valence band O2p to the conduction band Ti3d. The presence of reduced graphene or nitrogen-doped graphene is shifting the optical absorption edge towards the visible region. Additionally, a minimum reflectance level was obtained in the visible region for composites containing the graphene, the 20wt.% thermally reduced graphene having the largest impact. The catalyst with 10wt.% TRGO obtained by the first method has a lower absorption at 550 nm than the one obtained by the second method, showing a less efficient utilization of light by the present gold nanoparticles. Consequently, the 20wt% TRGO catalyst was prepared exclusively by the second method.

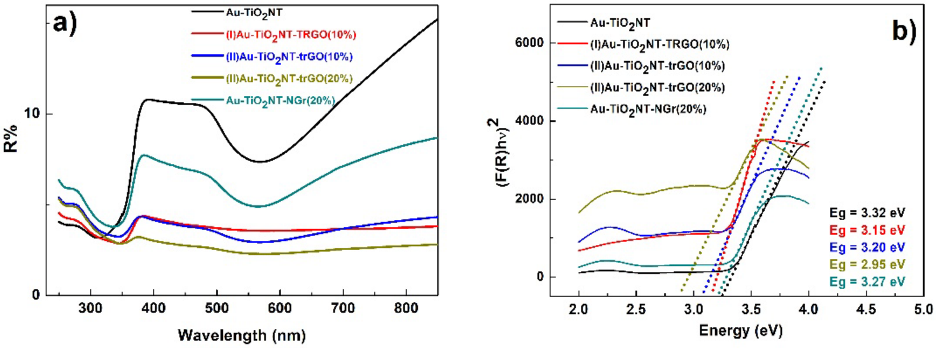

Figure 3. a). DR-UV–Vis spectra of Au-TiO_2NT-TRGO/NGr powders. b). The optical band gap estimation for Au-TiO_2NT-TRGO/NGr composites.

The diffuse reflectance (DRS) spectra were used to estimate the band gap (E_g) of the investigated photocatalysts, using Kubelka-Munk equation (Eq. 1) and the Tauc plot by representing the $[F(R)h\nu]^n$ *vs.* hv, where hv is the light energy (1240/λ), and n is the composite transition (direct transition, n = 1/2) [26].

$$F(R) = (1 - R_\infty)^2/(2R_\infty) \qquad (1),$$

where R_∞ represents the reflectance of the composite and F(R) is the absorbance.

The calculated band gap of each composite is presented in the Figure 3b. The bandgap of the starting TiO_2NTs was found to be 3.37 eV. A bandgap narrowing induced by the interfacial interaction among components was obtained for Au-TiO_2NT-TRGO/NGr composites. In accordance with previous studies [27, 28], these results proved that a more efficient utilization of light could be obtained and the Au-TiO_2NT-TRGO/NGr composites should possess higher photocatalytic efficiency than undecorated titania nanotubes for the degradation of organic pollutants, in the visible region.

Visible light photodegradation of amoxicillin

The composites containing gold nanoparticles and titania nanotubes prepared by the second method were tested for the influence of reduced graphene or nitrogen-doped graphene on the visible light-mediated photodegradation of amoxicillin, using white LED lamps in the domain 420 – 800 nm. For this, the adsorption and photocatalytic degradation processes were simultaneously studied. The adsorption equlibrium was set at one hour. The overall results of amoxicillin decrease (C/C_0), working with 1 mg/L amoxicillin and 0.5 mg/mL catalyst dose in a buffer phosphate at pH = 7 are shown in Figure 4. The presence of 10wt.%. reduced graphene oxide in the Au-TiO_2NT composite is not improving the photocatalytic behaviour. The decrease in amoxicillin concentration over exposure time was very similar (Figure 4, black and blue lines). The 20%wt. ratio of reduced graphene oxide or nitrogen-doped graphene is clearly enchancing the photocatalytic activity of Au-TiO_2NT composite. As expected, an even better response was measured for the nitrogen-doped graphene-containing composite (Figure 4, dark cyan line), most probably due to the presence of the free electrons of nitrogen atoms that are improving electronic transfer towards or from titania.

The adsorption stage is crucial for heterogeneous catalysis, as reactions are happening on the photocatalyst surface. Besides lowering the bandgap energy and enhancing the light absorption capability of the catalysts, the presence of 20% wt. of graphene (simple or nitrogen dopped) in the composites is leading to a larger amount of adsorbed amoxicillin, before exposure to light (Figure 4, dark cyan and dark yellow lines). In order to deepen the processes understanding, we performed a small study on the decrease of amoxicillin concentrations versus time during the adsorption process alone over a period of 120 minutes. Two starting concentrations of amoxicillin were employed: 1 mg/L and 1.5 mg/L. Data showed that an increase in the initial amoxicillin concentration is enhancing the adsorption (Figure 5). The initial adsorption rate is very rapid, then a bit slower and was not completely reaching the equilibrium, probably because the working concentrations were low and the maximum loading capacity of the photocatalysts cannot be achieved.

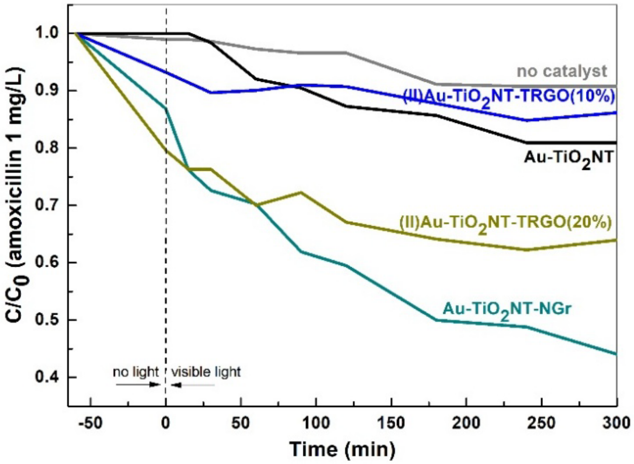

Figure 4. The decrease in amoxicillin ratio under visible light exposure using photocatalysts

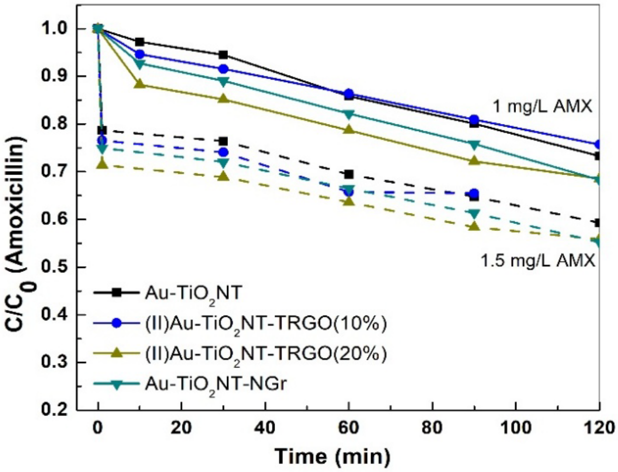

Figure 5. The decrease in amoxicillin ratio during adsorption stage on the selected photocatalysts

The kinetic study was performed by the linearization of the pseudo-first order, pseudo-second order and Elovich kinetic mathematical models of the obtained experimental data. The kinetic equations and parameters of the three models are described below:

$$\ln(q_e - q_t) = lnq_e - k_1 t \text{ (pseudo-first order model)} \tag{2}$$

$$t/q_t = 1/k_2 q_e^2 + t/q_e \text{ (second order model)} \tag{3}$$

$$q_t = \frac{1}{\beta}\ln(\alpha\beta) + \frac{1}{\beta}\ln t \text{ (Elovich model)} \tag{4}$$

where k_1 and k_2 are the corresponding rate constants, β is the desorption constant (g/mg) and α is the initial adsorption rate (mg/g min).

The calculated constants for the first two models are comparatively presented and the R-squared value are presented in Table 1 (the Elovich model fitting gave inconsistent results and are not presented here). The results show that the adsorption kinetic is dependent on the starting concentration. For all photocatalysts, the higher R^2 and the very close q_e experimental values show that the best describing model at 1 mg/L concentration is the pseudo-first order, while for a starting concentration of 1.5 mg/L the best describing model is the second order. This suggested that physical adsorption was the main process. The mechanism was similar for all the four measured photocatalysts, at small initial concentrations of amoxicillin. As expected, the concentration of graphene is influencing the adsorption. Reduced graphene is a known adsorbent and the catalyst with 20wt.% TRGO showed clearly the best adsorption of amoxicillin.

Table 1. Adsorption kinetics parameters for two concentrations of amoxicillin on the four selected photocatalysts

Composite	**Initial AMX conc. (mg/L)**	**q_e exp.** (mg/g)	**Pseudo-first order model**			**Second order model**		
			q_e (mg/g)	k_1 (min^{-1})	R^2	q_e (mg/g)	K_2 (mg/(g . min))	R^2
Au-TiO_2NT	1	0.55	0.59	0.015	0.9680	0.93	0.0092	0.2978
	1.5	1.03	-	-	0.5620	1.01	0.1212	0.9590
(II)Au-TiO_2NT-TRGO(10%)	1	0.50	0.50	0.016	0.9729	0.57	0.0459	0.7648
	1.5	1.26	-	-	0.6762	0.91	0.2385	0.9847
(II)Au-TiO_2NT-TRGO(20%)	1	0.64	0.61	0.022	0.9558	0.694	0.0726	0.9112
	1.5	1.12	-	-	0.4980	1.157	0.1049	0.9825
Au-TiO_2NT-NGr	1	0.66	0.65	0.014	0.9810	0.742	0.0356	0.7568
	1.5	1.12	-	-	0.5770	1.163	0.0715	0.9591

Further on, the photodegradation step of amoxicillin, under visible light irradiation, was also evaluated from the kinetic point of view in order to evaluate the amoxicillin removal in time. It is generally accepted that photocatalytic reactions are following the simplified Langmuir-Hinshelwood model of pseudo-first order kinetics described by equation (5) [29].

$$r = -\ln\left(\frac{C}{C_0}\right) = k_{obs}t \qquad (5)$$

where r is the reaction rate, C is the amoxicillin concentration and k_{obs} the observed first order rate constant.

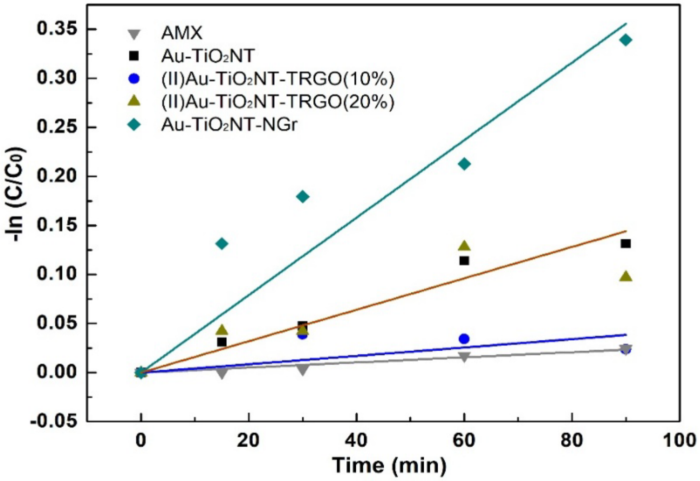

Figure 6. Liniarization of amoxicillin photodegradation following the 1st order kinetics model

Figure 6 presents the linear fitting of the representation of -ln(C/C_0) as a function of time for the four selected photocatalysts, on the time interval up to 90 minutes. The obtained values for the apparent velocity constant (k_{obs}) of 0.00042 min^{-1} (for (II)Au-TiO$_2$NT-TRGO(10%)), 0.0016 min^{-1} (for Au-TiO$_2$NT and (II)Au-TiO$_2$NT-TRGO(20%)) and 0.0039 min^{-1} (for Au-TiO$_2$NT-NGr) show that Au-TiO$_2$NT-NGr composite was photodegrading the amoxicillin the fastest. This observation is in contradiction with the observed modifications in the optical properties of the investigated materials, that measured narrower bandgaps for the catalysts bearing reduced graphene oxide instead of nitrogen-doped graphene. The larger reaction rate associated with the nitrogen-doped can only be explained by the reported enhanced electronic mobility between TiO$_2$ and graphene [21,22].

CONCLUSIONS

This work demonstrated the efficient decoration of titania nanotubes with gold nanoparticles (around 20 nm) and introduction of reduced graphene oxide (up to 20%wt.) or nitrogen-doped graphene, by two preparation methods. These improved the optical properties of the photocatalyst by narrowing the band gap energy value and enlarging the visible light absorption capabilities. The combined effects led to better photocatalytic performances in the removal of amoxicillin (up to 60%) under visible light irradiation, mediated by the nitrogen-doped containing photocatalyst. This is probably due to the electron mediator role of nitrogen-doped graphene, providing an efficient separation between the photogenerated electrons in TiO_2 and photogenerated holes in Au. This study confirms the importance of the graphene presence in the composition of photocatalysts for the visible-light mediated processes, leading to a more efficient use of solar light for environmental applications.

EXPERIMENTAL SECTION

Materials and methods

The starting TiO_2 nanotubes were received from USN, Norway and were prepared by hydrothermal method. Graphene oxide was prepared according to the reported literature procedure [19]. The NGr_{int} was prepared according to the reported literature procedure [18]. Au(2.5%)-TiO_2NT were prepared according to the reported literature protocol [17]. Amoxicillin and HPLC-grade formic acid were purchased from Sigma-Aldrich.

Scanning/Transmission Electron Microscopy (STEM) was employed to investigate the morphology of the composites (at 200 kV and 10 µA) using an H-7650 120 kV Automatic Microscope (Hitachi, Japan). The samples were prepared by dropping a few µL of diluted ethanol suspension of the composites on the copper grid.

The diffuse reflectance UV–Vis spectra of Au-TiO_2NT-containing composites were recorded on a V-570 JASCO Spectrophotometer using solid powders. X-Ray powder Diffraction (XRD) measurements were performed on a Bruker D8 Advance diffractometer, using CuKα1 radiation (λ = 1.5406 Å), with 0.02 grade 2θ/second.

Preparation of (I)Au(2.5%)-TiO_2NT-TRGO(10%)

TiO_2NT, together with the appropriate amount of graphene oxide (GO) were impregnated with an appropriate volume of 0.076 M $HAuCl_4$ solution to result into a 2.5%wt. gold(0). The slurry was dried under normal conditions and the resulted solid was heated up to 250°C under argon flow, and then the gas flow was switched to a mixture of H_2 in Ar (10 vol.% H_2) in order to pursue the reduction of graphene oxide (250°C, 10 minutes), resulting into Au-TiO_2NT with thermally reduced graphene oxide, denoted as (I)Au(2.5%)-TiO_2NT-TRGO(10%).

Preparation of (II)Au(2.5%)-TiO_2NT-TRGO

Au(2.5%)-TiO_2NT was sonicated with the appropriate amount of graphene oxide (GO) followed by lyophilization. The resulted composite was seated in a quartz boat into a temperature-programmed furnace. The furnace was heated up to 250°C under argon flow, and then the gas flow was switched to a mixture of H_2 in Ar (10 vol.% H_2) in order to pursue the reduction of graphene oxide (250°C, 10 minutes), resulting into Au-TiO_2NT with thermally reduced graphene oxide, denoted as (II)Au(2.5%)-TiO_2NT-TRGO(10%) and (II)Au(2.5%)-TiO_2NT-TRGO(20%).

Preparation of Au(2.5%)-TiO_2NT-NGr

Au(2.5%)-TiO_2NT was sonicated with the appropriate amount of NGr_{int}, followed by lyophilization. The resulted solid was heated up to 500°C under argon flow, resulting into Au-TiO_2NT with nitrogen-doped graphene, denoted as Au(2.5%)-TiO_2NT-NGr(20%).

Adsorption and photocatalytic degradation of amoxicillin

The photocatalytic degradation tests were carried out in a Photoreactor Luzchem LZC-4V (Canada) equipped with 12 white LEDs (8 W) that emits in the visible domain 420 – 800 nm, the light intensity being 241.000 lx (lumen/m^2). The batch equilibrium experiments (adsorption/desorption) were performed in the dark over the described period of time (60 minutes or 120 minutes). After adsorption, the visible light was turned on and 150 µL aliquots were withdrawn from the solutions at various time intervals under well-mixing conditions and transferred to an inset in a two-mL HPLC vial and the aqueous concentration of amoxicillin was determined by a high-performance liquid chromatograph (HPLC) equipped on a UHPLC Restek Pinnacle C18 column (5 × 2.1 mm; 1.9 µm particle size) at room temperature, isocratic elution acetonitrile: water (0.3% formic acid) = 95:5 at a flow rate of 0.25 mL/min, and the UV detector set at 230 nm. Amoxicillin concentrations were calculated on the basis of a calibration curve.

The residual ration (C/C_0) were calculated with the following formula:

$$\frac{C}{C_0} = \frac{C_t}{C_i} \tag{6}$$

ACKNOWLEDGMENTS

This work was supported through the “Nucleu” Program within the National Research Development and Innovation Plan 2022–2027, Romania, carried out with the support of MEC, project no. 27N/03.01.2023, component project code PN 23 24 01 01.

REFERENCES

1. A. Malik, E. Grohmann, *Environmental Protection Strategies for Sustainable Development*, Springer Netherlands, 2012, p. 12
2. S.C. Ameta, R. Ameta, *Advanced oxidation processes for waste water treatment-emerging green chemical technology*, *Chapter 6 – Photocatalysis*, Academic Press, 2018, 135-175
3. N. Farooq, P. Kallem, Z. ur Rehman, M. I. Khan, R. K. Gupta, T. Tahseen, Z. Mushtaq, N. Ejaz, A. Shanableh, Recent trends of titania (TiO_2) based materials: A review on synthetic approaches and potential applications, *Journal of King Saud University – Science* **2024**, *36*, 103210.
4. O. Carp, C.L. Huisman, A. Reller, *Prog Solid State Ch* **2004**, *32*, 33–177
5. M. Pelaez, N.T. Nolan, S.C. Pillai, M.K. Seery, P. Falaras, A.G. Kontos, P.S.M. Dunlop, Jeremy, W.J. Hamilton, J.A. Byrne, K. O’Shea, M.H. Entezari, D.D. Dionysiou, *Appl Catal B* **2012**, *125*, 331-349
6. M.J. Wu, T. Bak, P.J. O’Doherty, M.C. Moffitt, J. Nowotny, T.D. Bailey, C. Kersaitis, *Int J Photochem* **2014**, 1-9
7. T. Umebayashi, T. Yamaki, H. Itoh, K. Asai, *J Phys Chem Solids* **2002**, *63*, 10, 1909-1920
8. S. Linic, P. Christopher, D.B. Ingram, *Nat Mater* **2011**, *10*, 12, 911-921
9. E. Bae, W. Choi, J. Park, H.S. Shin, S. Bin Kim, J.S. Lee, *J Phys Chem B* **2004**, *108*, 37, 14093-14101
10. H. Park, Y. Park, W. Kim, W. Choi, *J Photochem Photobiol C: Photochem Rev* **2013**, *15*, 1-20
11. M. Minella, D. Fabbri, P. Calza and C. Minero, *Curr Opin Green Sust Chem* **2017**, *6*, 11–17
12. S.D. Perera, R.G. Mariano, K. Vu, N. Nour, O. Seitz, Y. Chabal Jr, K.J. Balkus, *Catalysis* **2012**, *2*, 949–956
13. J. Liu, H. Bai, Y. Wang, Z. Liu, X. Zhang, D.D. Sun, *Adv Funct Mater* **2010**, *20*, 23, 4175–4181
14. A. Trapalis, N. Todorova, T. Giannakopoulou, N. Boukos, T. Speliotis, D. Dimotikali, J. Yu, *Appl Catal B* **2016**, *180*, 637–647
15. A. Urda, T. Radu, C. Socaci, V. Floare-Avram, D. Cosma, M. C. Rosu, M. Coros, S. Pruneanu, F. Pogacean, *J. Photochem. Photobiol. A* **2022**, *425*, 113701.
16. D. Cosma, A. Urda, T. Radu, M.C. Rosu, M. Mihet, C. Socaci, *Molecules* **2022**, *27*, 18, 5803.

17. D. Cosma, M.-C. Roşu, C. Socaci, A. Urda, T. Radu, A. Turza, M. Dan, R. M. Costescu, K. R. Gustavsen, O. Dobroliubov, K. Wang, *Journal of Environmental Chemical Engineering* **2024**, *12*, 3, 112885.
18. A. Urda, T. Radu, K. R. Gustavsen, D. Cosma, M. Mihet, M. C. Rosu, A. Ciorîța, A. Vulcu, K. Wang, C. Socaci, How is graphene influencing the electronic properties of NiO-TiO2 heterojunction?, *Journal of Physics D: Applied Physics* **2025**, *58*, 015103.
19. A.T. Kuvarega, B.B. Mamba, *Crit Rev Solid State Mater Sci* **2016**, 295-346
20. P. Huo, P. Zhao, Y. Wang, B. Liu, M. Dong, *Energies* **2018**, *11*, 630
21. H. Pan, X. Zhao, Z. Fu, W. Tu, P. Fang, H. Zhang, *Appl Surf Sci* **2018**, *442*, 547–555
22. H. Xu, M. Ding, W. Chen, Y. Li, K. Wang, *Sep Purif Technol* **2018**, *195*, 70–82
23. D. Ding, B. Wang, X. Zhang, J. Zhang, H. Zhang, X. Liu, Z. Gao, Z. Yu, *Ecotoxicol. Environ. Saf.* **2023**, *254*.
24. S.M. Al-Jubouri, H.A. Sabbar, E.M. Khudhair, S.H. Ammar, S. Al Batty, S. Yas Khudhair, A.S. Mahdi, *J. Photochem. Photobiol. A Chem.* 2023, *442*.
25. J. Liu, K.Y. Chen, J. Wang, M. Du, Z.Y. Gao, C.X. Song, *Journal of Chemistry* **2020**, 2928189.
26. P. Martins, S. Kappert, H.N. Le, V. Sebastian, K. Kühn, M. Alves, L. Pereira, G. Cuniberti, M. Melle-Franco, S. Lanceros-Méndez, *Catalysts* **2020**, *10*, 234.
27. N. Liu, X. Chen, J. Zhang, J.W. Schwank, *Catalysis Today* **2014**, *225*, 34– 514.
28. D. Chen L. Zou, S. Li, F. Zheng, *Scientific Reports* **2016,** *6*, 20335.
29. C. Turchi, D.F. Ollis *J. Catal.* **1990**, *122*, 178–192.